STRUCTURE, PHASE TRANSFORMATIONS, AND DIFFUSION

Wear Performances of Hypereutectoid P/M Steels Subjected to Different Heat Treatments

Ahmet Güral[a,]*, Kevser Ceyda Taşkıran[b, c], Onur Altuntaş[d], and Tolga Yılmaz[a, c]

[a] Gazi University, Department of Metallurgical and Materials Engineering, Faculty of Technology, Ankara, Turkey
[b] Turkish Aerospace, Department of Patent Engineering, Ankara, Turkey
[c] Gazi University, Graduate School of Natural and Applied Sciences, Metallurgical and Materials Engineering, Ankara, Turkey
[d] Department of Warfare Weapons and Tools, Alparslan Defense Sciences and National Security Institute, National Defense University, Ankara, Turkey
*e-mail: agural@gazi.edu.tr

Abstract—Dry sliding wear test specimens of high-carbon powder metallurgy steels were performed in accordance with the ASTM G99-05 standard. Heat treatment of sintered specimens was carried out by the austenitization process at 950°C for 4 min, next quenching in a salt bath at 210, 350 and 400°C for 60–360 s. Wear performances of the specimens were carried out with a constant load of 10 N, at a sliding speed of 1.00 m s^{-1} and up to a sliding distance of 1000 m. Scanning electron microscopy (SEM) and X-ray diffraction (XRD) were used for microstructure analysis and phase identification. It was seen that the friction coefficient of the specimen was not directly related to the hardness. The friction coefficient of the specimen with the lowest hardness, which was treated isothermal at 400°C, is lower than the specimen with higher hardness. However, even though the friction coefficient is low in this sample, the increase in the wear rate was remarkable. In other specimens, the coefficient of friction and wear rate decreased proportionally with the increase in their hardness. The wear rate of the specimens was reduced by the decrease in isothermal holding temperature and time.

INTRODUCTION

The ferrous alloys containing 2 wt % C are used in various industrial applications that require high strength and excellent wear resistance [1–3]. Primary cementite surrounding pearlite colonies in the microstructure of steels with hypereutectoid composition damage the ductility and mechanical properties of these steels [4, 5]. While the increase in carbon content causes the martensite transformation start (M_s) and martensite transformation finish (M_f) temperatures to decrease, the probability of retained austenite formation between martensite plates increases when quenching is applied for hardening. The retained austenite increases by the quenching rate and alloying elements [6, 7]. As these contain more dislocations and other crystal defects, they cause increased internal stresses. Hence it is an undesirable micro-formation since it can cause cracks and fractures during the use of steel containing retained austenite. In order to prevent this adverse situation, austempering and martempering processes can be offered especially for high-carbon steels [8–10]. A typical austempering is simply to produce a bainitic structure by keeping it at a constant temperature above the M_s temperature until the bainite transformation finish (B_f) time, according to the temperature-time-transformation (TTT) diagram of the steel. According to the TTT diagram, martempering is used to produce unstressed martensite by holding it at a constant temperature just above the M_s temperature until the bainite transformation start time (B_s) [6].

Material production by powder metallurgy is among important manufacturing methods. Typically, for the desired alloy design, powders of different chemical compositions are mixed into the main powder and sintered at high temperatures to form diffusion bonds and dissolve the alloying elements [11–13]. Nowadays powder metallurgy materials are used in many fields such as mechanical manufacturing, automotive, and aerospace industries etc. [14–18]. Power transmission and bearing materials produced by powder metallurgy have an important place. Also, heat treatments are applied to produced parts in order to improve mechanical and wear properties [19–22]
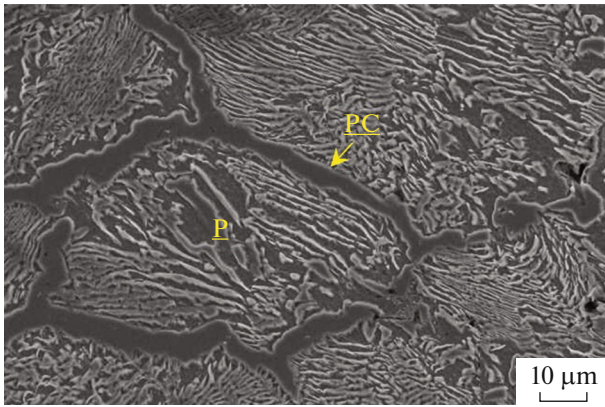
Fig. 1. As-sintered SEM microstructure with primary cementite (PC) phase plus pearlitic (P) structure.

Since parts produced by the conventional powder metallurgy method contain pores, heat treatments should be applied carefully. In order to reduce the heat treatment quenching rate, it is mostly preferred to increase the additions of alloying elements [23, 24]. However, such a method can significantly increase the cost of production.

In the present study, high-carbon powder metallurgy steel specimens were produced without adding alloying elements. By the different isothermal holding temperature and time, austempering and martempering heat treatments, which can be safer for mechanical/wear properties, were applied instead of traditional quenching heat treatment. Thus, dry sliding wear properties of powder metallurgy steels martempered heat treatment, which had not been applied before were investigated in comparison with the austempering processes.

EXPERIMENTAL

To produce high C powder metallurgy steel, 1.5 wt % natural graphite powder was added to pure iron powder (ATOMET 1001-Höganäs). Green wear test specimens with a diameter of 10 mm and a height of 15 mm in accordance with ASTM G99-05 standards were produced from mixed powders by cold compaction under 700 MPa pressure in a die. Compacted wear specimens were sintered under 99.99% purity Argon gas atmosphere at 1200°C for 20 min. Green and sintered densities of the specimens were achieved with an Archimedes density meter and found to be 6.9 and 7.2 g cm^{-3}, respectively. For the heat treatment of sintered specimens, the first austenitization process was carried out at 950°C for 4 min, then quenched in a salt bath at 210, 350 and 400°C, isothermal annealing for 60−360 s and quenched again in water at room temperature. According to these procedures, the specimens were coded with the "IQ" symbol indicating isothermal annealed plus quenched, the first three-digit

number representing the temperature and the next number representing the holding time. As explained in the example, according to the IQ210-180 coding, it was annealed and quenched at 210°C for 180 s.

Specimens were conventionally sandpapered, polished, and then etched in 3% nital solution to reveal microstructures. JEOL JSM-6060LV SEM was used to image the microstructures. APD 2000 PRO-XRD brand X-ray diffraction (XRD) Instrument in order to identify phases in specimens and has been carried out using Cu$K\alpha$ radiation (λ = 1.5418 Å) and scans in 2θ between 20° and 90° with 0.02 steps.

The HV1 Vickers hardness values of the specimens were determined with the SHIMADZU HVM2 hardness tester. The mean values were calculated by measuring the hardness from at least five different points in each specimen. The dry sliding wear tests of the specimens were carried out on the TRIBOMETER T10/20 wear tester in accordance with the ASTM G99-05 standard. The disc used as abrasive surface is steel having a hardness of 55 HRC. All dry sliding wear tests were carried out under a constant load of 10 N, at a sliding speed of 1.00 m s^{-1} and up to a sliding distance of 1000 m. As a result of the wear test, average weight losses of the specimens were determined on a 0.1 mg precision scale. Then, the volume ratio (m^3) was calculated from the mass loss and the wear rate in m^3 (N m)$^{-1}$ was determined by considering the applied load (N) and the sliding distance (m). In addition, the friction coefficient was automatically recorded by the software to which the system was connected. Worn surfaces of the specimens were imaged by SEM.

RESULTS AND DISCUSSION

In Fig. 1, the microstructure obtained after the sintering process is given. As expected, primary cementite (PC) networks formed continuously at grain boundaries of pearlite colonies since it has a hypereutectoid carbon composition. It was observed that perlite colonies containing the secondary cementite phase were formed in divorced morphology. In alloys having hypereutectoid carbon composition, the network dispersion of the PC phase in the structure damages many mechanical properties of the steel, such as ductility, ultimate tensile strength, and toughness. One of the other hardness increasing methods to improve wear properties is to produce a martensitic phase by quenching. The plate type fully martensitic microstructure was achieved when quenched directly. However, internal cracks (IC) were caused when the high-C specimens were rapidly quenched after austenitizing at 950°C as seen in Fig. 2.

Austenite grain size and C content cooling rate before quenching was important consideration in martensite cracking. Coarse austenite grain size has been reported to induce quenching cracking [25]. In addition, long and wide martensite plates are prone to
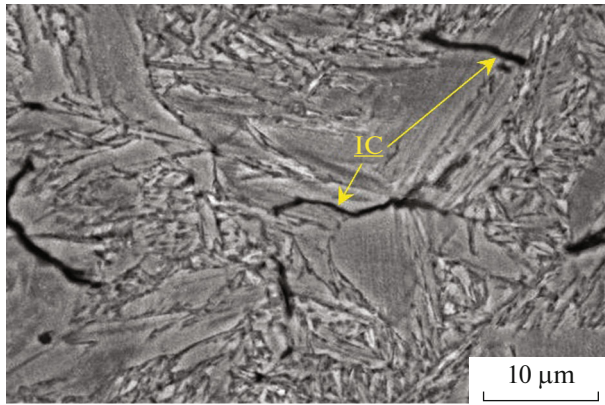
Fig. 2. As-quenched SEM microstructure having high carbon plate type martensitic with internal cracking (IC) subsequent sintering process.

cracking has been reported. There may be microcracks at the interface during the distortion of the plates [26]. Retained austenite may also be responsible for this situation.

In order to prevent internal microcracks in martensite plates during quenching in high-carbon steels as seen in Fig. 2, martempering heat treatments are rec-

ommended. This process is used to produce the martensite phase by quenching below M_s and M_f temperatures before isothermal holding above the M_s transformation temperatures of the austenitized steel and before the bainitic transformation begins. By this way, residual stress is avoided [6, 27].

In Fig. 3, microstructures of the specimens, which were subjected to martempering according to different holding times at 210°C, are presented. When martempering is performed at 210°C for 30 s, the presence of quenching cracks is still observed (Fig. 3a). The presence of a typical tempered martensite structure in the IQ210-30 and IQ210-90 specimens can be noted up to 30 and 90 s isothermal holding time (Figs. 3a and 3b). The process performed on the IQ210-90 specimen was verified as martempering process. When the TTT diagram of a plain C steel with a high C hypereutectoid is examined as shown in Fig. 4, it can be observed that martensitic transformation can be achieved in martempering processes performed at 210°C for up to 100 s (red line in Fig. 4). When the holding time at this temperature exceeds 100 s, the presence of partial martensite phases and bainitic transformations can be formed in the IQ210-180 specimen as seen in Fig. 3c. Probably, the holding time of the IQ210-180 specimen with martensitic plus bainitic microstructures is
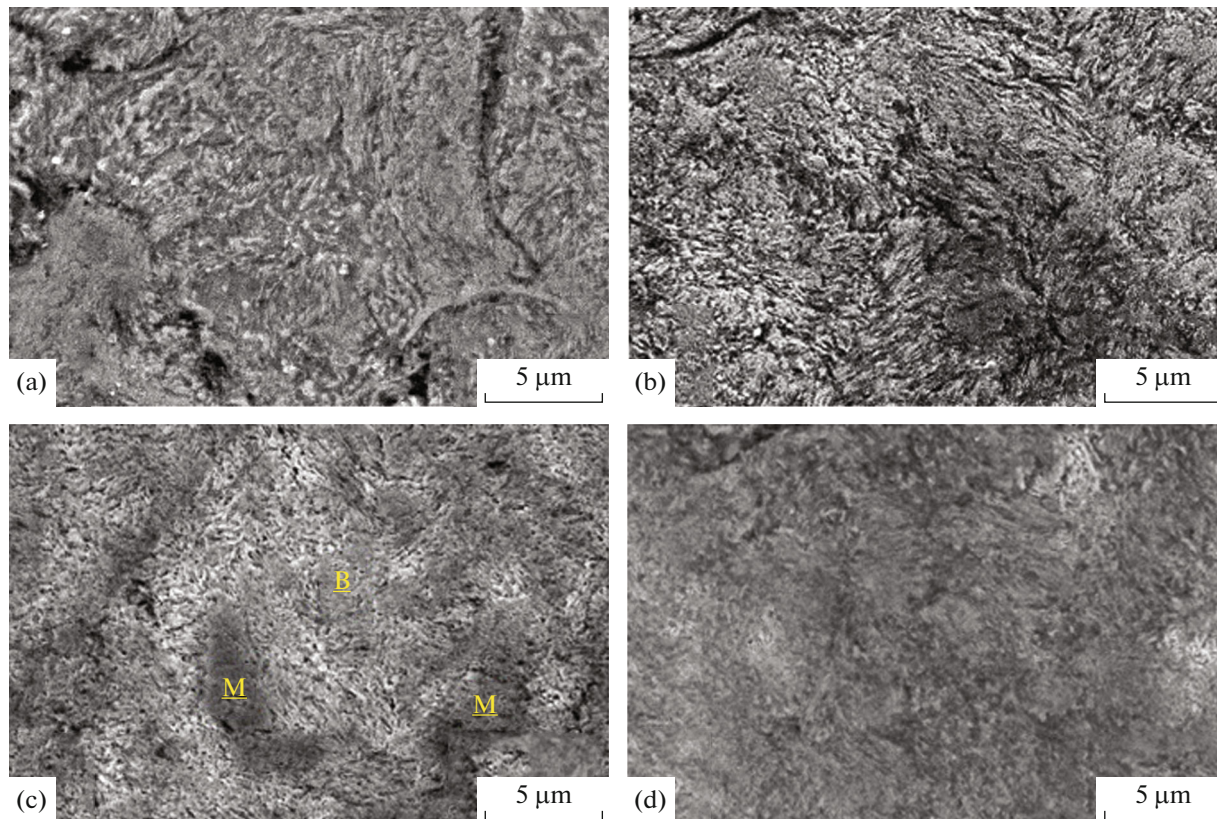

Fig. 3. Microstructure evaluations depending on isothermal holding time at 210°C of the (a) IQ210-30, (b) IQ210-90, (c) IQ210-180 and (d) IQ210-360 (IC: Internal cracking M: Martensite, B: Bainite).
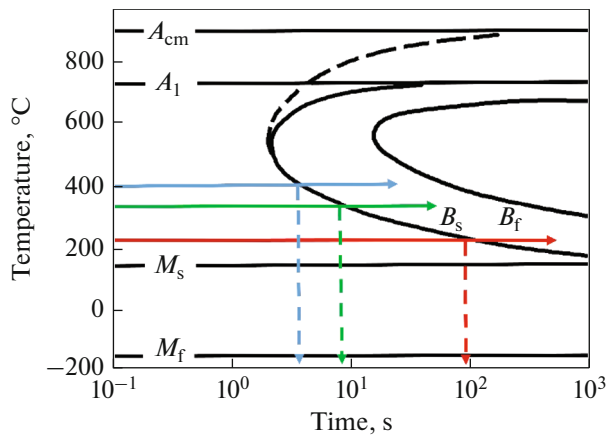
Fig. 4. TTT diagram of hypereutectoid carbon steel [28].

between bainite transformation (B_s) and bainite finish (B_f) in the TTT diagram shown in Fig. 4. In the IQ210-360 specimen, when the isothermal holding time at 210°C was 360 s, a complete bainitic transformation occurred in the microstructure (Fig. 3d).

In Fig. 5, microstructures of the specimens kept isothermal at 350°C for different periods are shown. It can be seen that the bainitic transformation begins when it is kept at this temperature for 30 s in the IQ350-30 specimen (Fig. 5a). As shown by the green line on the TTT diagram in Fig. 4, the bainitic transformation starts in 10 s at 350°C. Bainitic plus lamellar pearlitic structures are formed when the holding time is increased in the IQ350-90 and IQ350-180 specimens (Figs. 5b and 5c). According to the TTT diagram, the martempering time is shortened even more when isothermal processes are applied at 400°C (blue line). It is the upper bainitic structure of the microstructure in the IQ400-60 and IQ400-90 specimens obtained by 60 and 90 s isothermal treatment applied at this temperature (Figs. 6a and 6b). Upper bainite region characterized by parallel aligned ferrite laths are shown in Fig. 6. In the typical upper bainite microstructure, ferrite laths are characterized by being separated by cementite precipitates [29].

The process, known as martempering, can both prevent the formation of residual austenite formed during severe quenching, and reduce the risk of distortion and cracking. In powder metallurgy materials, it is inevitable that internal pores also have a notch effect. This, in particular, plays a role in accelerating quenching cracks used for hardening. Therefore, martempering in high-carbon powder metallurgy steels is recommended to improve many mechanical and tribological properties of the material.
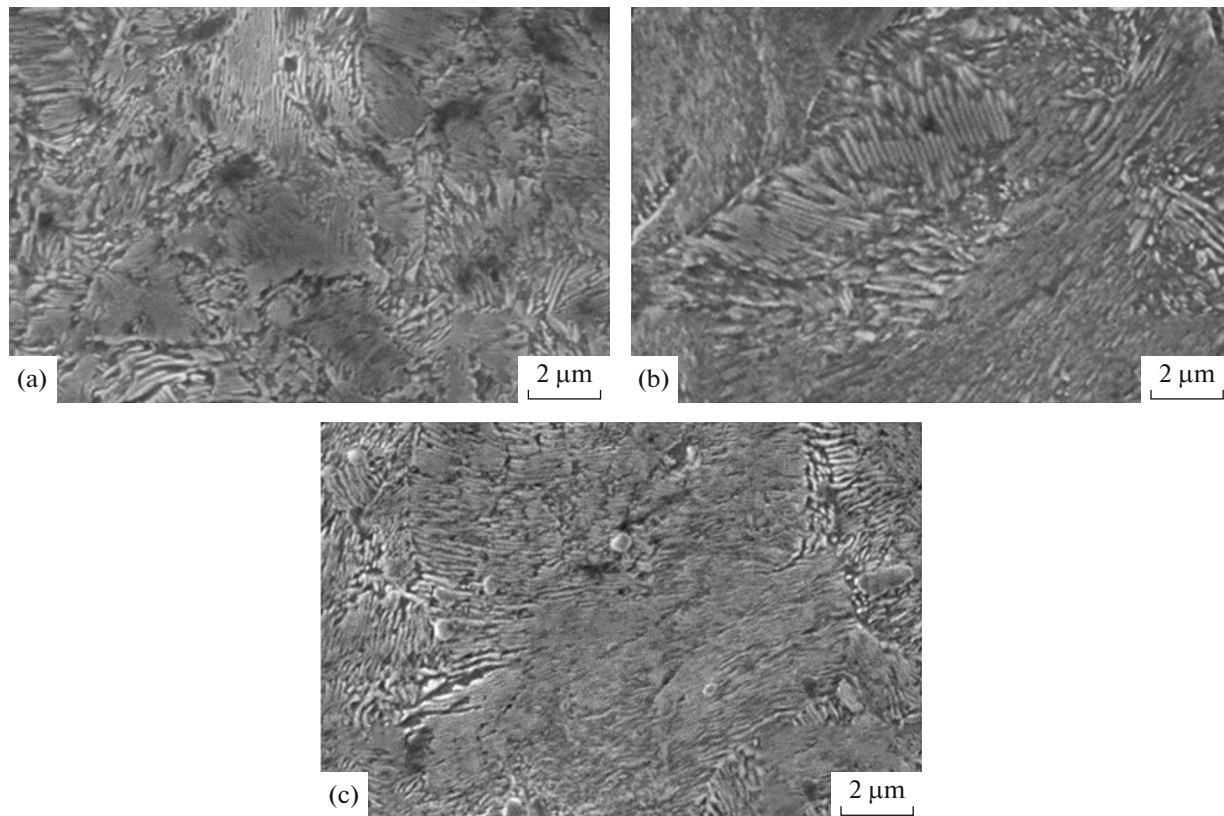

Fig. 5. Microstructure evaluations depending on isothermal holding time at 350°C of the (a) M350-60, (b) M350-90 and (c) M350-180 specimens.
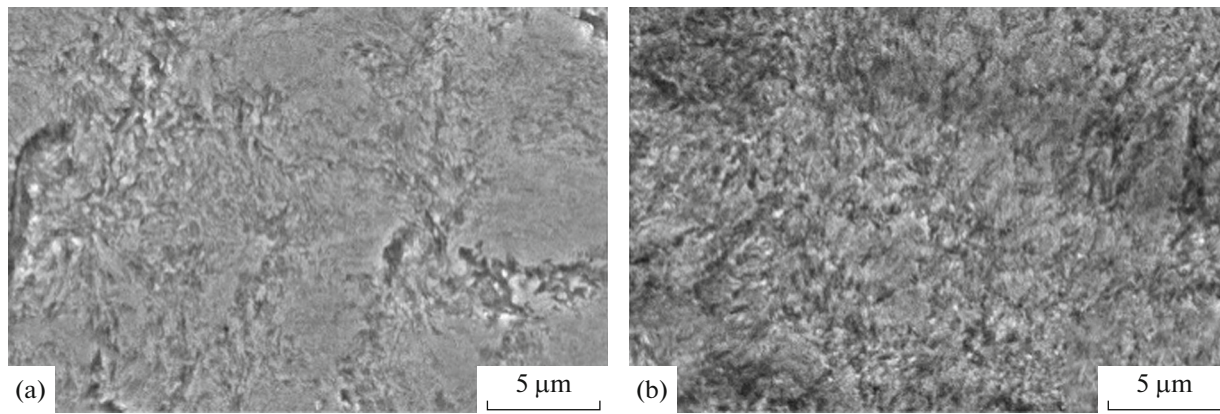
Fig. 6. Microstructure evaluations depending on isothermal holding time at 400°C of the (a) IQ400-60 and (b) IQ400-90 specimens.

Retained austenite can cause serious problems, especially in high C steels. It increases internal stresses in mechanical or tribological working conditions and it can cause tempering embrittlement. XRD pattern analyses of the specimens are given in Fig. 7. In the XRD analysis of the as-quenched specimen, the presence of untransformed austenite peaks in the (111), (200), and (220) planes can be clearly seen (Fig. 7a). It can be understood from the XRD patterns that these intensities have decreased significantly in specimens that were kept isothermal and quenched at different temperatures and times specimens (Figs. 7b–7f). As the amount of C increases, the Ms and Mf temperatures required for martensite transformation decrease further. This situation leads to a further increase in the amount of retained austenite. It is reported that the residual amount of directly quenched austenite can be eliminated by tempering or secondary tempering [6]. As seen Figs. 7b–7f, it has been clearly demonstrated that marquenching and austempering treatment contributes to the reduction of retained austenite in high C powder metallurgy materials. By transforming the retained austenite to martensite, the dimensional stability of the steel is ensured and the hardness and wear properties are improved in a precisely way [30]. According to the XRD pattern of the IQ210-60 specimen in Fig. 7b, the amount of retained austenite has decreased significantly even with the martempering at a low temperature of 210°C for 60 s. The presence of residual austenite was similarly eliminated by increasing the isothermal holding and quenching temperature for a shorter time in the IQ350-30 and IQ350-60 specimens (Figs. 7c, 7d). XRD analysis results of the IQ400-30 and IQ400-60 specimens revealed that Fe_3C (cementite) formations occurred by increasing the high temperature (350–400°C) for longer isothermal holding time (60 s) by austempering processes (Figs. 7d–7f). This reason is explained as follows, as can be seen in Fig. 4, Fe_3C micro formation starts in addition to austenite at 350 and 400°C in a longer time (when the B_s time is exceeded). When quenched, Fe_3C

formation can be expected as bainitic transformation takes place with martensite.

In Fig. 8, the HV1 hardness value graph is presented depending on different isothermal temperatures and times. As the isothermal temperatures decreased, the hardness value increased as expected. While the hardness value was 370 HV1 in the IQ210-90 specimen, which was annealed 90 s at 210°C, it decreased to 340 HV1 in the IQ210-360 specimen, where the isothermal holding time was 360 s. It can be understood that the Bs time is approximately 100 s, as indicated by the red straight arrow at 210°C in the schematically TTT diagram of 1.2% C steel in Fig. 4. Therefore, it can be understood that this treatment of the IQ210-90 specimen is completely in martempering conditions. In the IQ210-180 and IQ210-360 specimens, the Bs time is exceeded since the isothermal holding time is 180 and 360 s. As indicated by the dashed red arrow in Fig. 4, when quenching occurs during this time interval, a decrease in hardness values is expected since the formation of bainitic structures
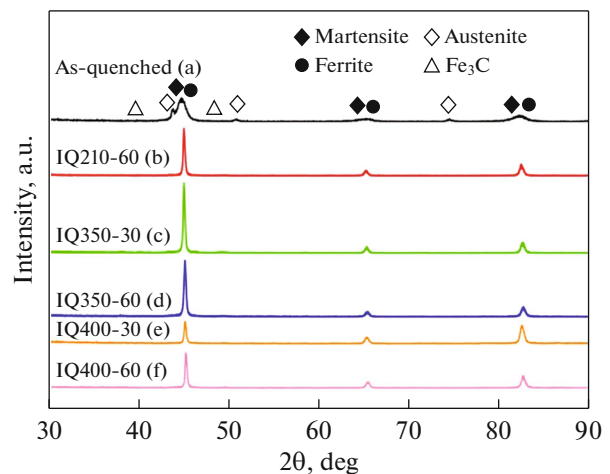

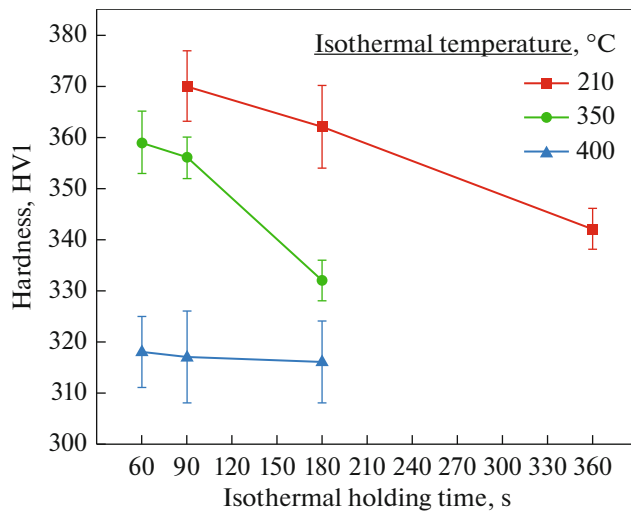**Fig. 7.** XRD pattern analyses of the specimens.

Fig. 8. HV1 hardness graph of isothermally annealed and quenched specimens at different temperatures and times.

with martensite in the microstructure occurs. Since the isothermal holding time of 360 s in the IQ210-360 specimen could not reach the Bf time at this temperature, the hardness value decreased due to the presence of bainite structure and less martensite phase in the microstructure. With the increase of isothermal holding temperatures in IQ350 and IQ400 specimens, the Bs conversion time decreased to about 10 s and below. Therefore, since bainitic transformation took place earlier in these specimens, the HV1 hardness values were lower than the IQ210 series specimen. While the hardness values obtained in IQ 350-60 and IQ400-60 specimens, which were kept isothermal for 60 s, were 360 HV1 and 320 HV1, respectively, it was determined that they were 330 and 315 HV1, respectively, at the

end of 180 s holding time at the same temperatures in the IQ350-180 and IQ400-180 specimens. It is a typical austempering process to produce upper bainite at the end of the temperature and time treatment applied on IQ350 and IQ400 specimens. The microstructure essentially has more toughness properties, especially under dynamic loads, with a partial decrease in hardness and a significant increase in ductility. On the other hand, martempering heat treatment can be preferred by minimizing internal stresses, as in the IQ210-90 specimen, which exhibits more hardness, especially in order to improve wear resistance in static loads such as bearing materials. The main purpose of the study is to provide as high a hardness value as possible without residual stresses or quenching cracks.

In Figs. 9 and 10, the friction coefficient (μ) and wear rates of the specimens depending on the isothermal holding time and temperatures are given, respectively. As seen in Fig. 9, there is an increase in friction coefficient values with the increase in isothermal holding time. This situation can be associated with hardness values of the specimens. When the hardness values decrease, it can be noted that the adhesive friction mechanism is more effective under dry friction conditions. On the other hand, it is noteworthy that the coefficient of friction decreases when the isothermal holding temperature is 400°C.

It is thought that this situation reduces the contact area in the counter material where Fe_3C precipitates in the microstructure come into contact, as upper bainite formation occurs at the end of the isothermal holding time at this temperature, as shown schematically in Fig. 11. In the case of the upper bainite microstructure, the slightly coarsened Fe_3C material may protrude slightly on the outer surface due to its high hardness. Because the soft ferritic matrix initially moves
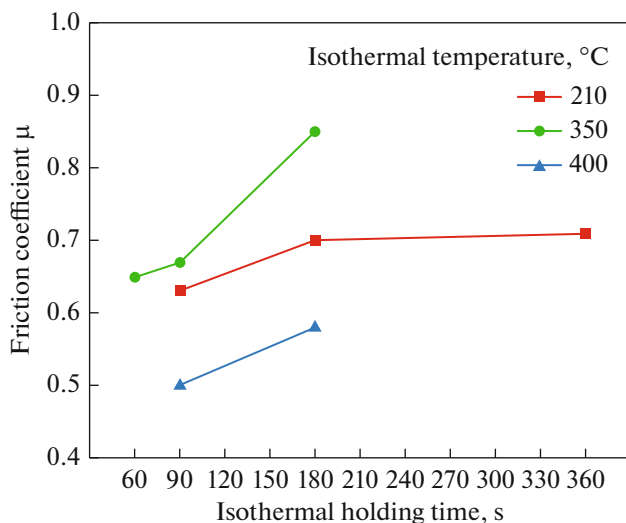

Fig. 9. Friction coefficient variation depending on the isothermal holding time and temperature of the specimens.
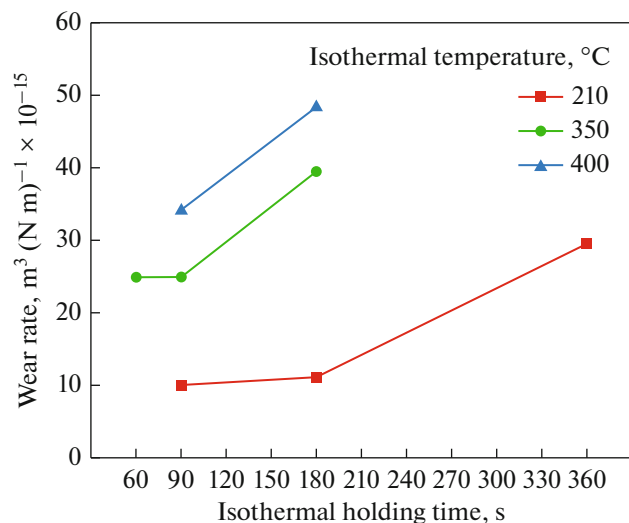

Fig. 10. Wear rate variation depending on the isothermal holding time and temperature of the specimens.
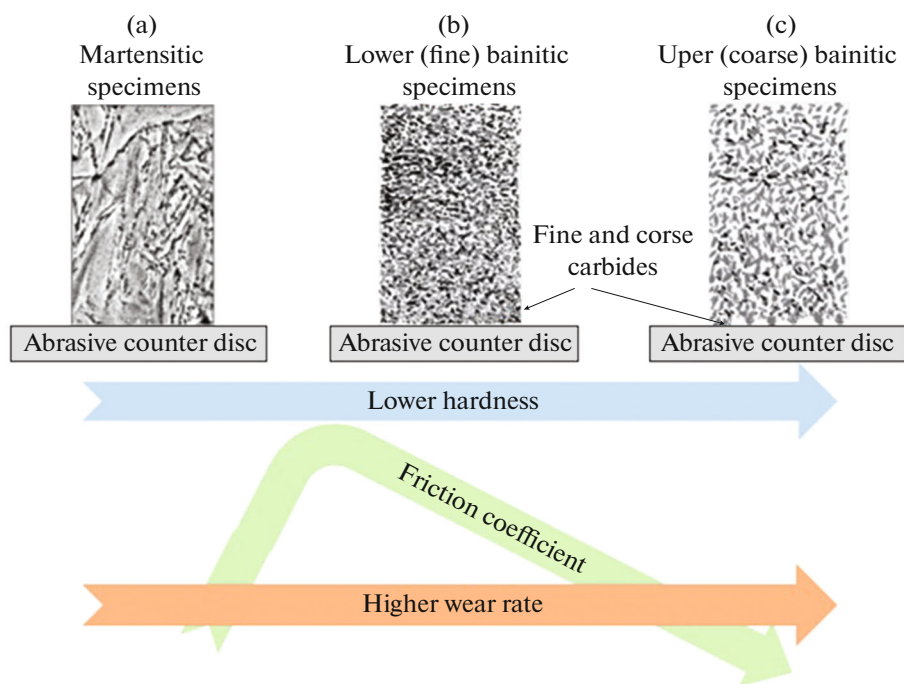
Fig. 11. Schematically the contact status of (a) martensitic, (b) finer bainitic and (c) coarser bainitic microstructures to the counter material disc.

away from the material during friction. Then the protruding Fe_3C phase can reduce the contact surface ratio. Thus, it can be noted that the coefficient of friction decreases. Since the more homogeneous lower bainite and martensite microstructures have more surface contact area, the friction coefficient is controlled by the hardness of the material in this case.

While the lowest friction coefficient was $0.51-0.59$ in IQ400-60 and IQ400-90 specimens, the highest friction coefficient values were 0.65 and 0.85 in IQ350-60 and IQ350-180 specimens, respectively. It can be noted that the coefficient of friction in these specimens increases more effectively with the isothermal holding time. The friction coefficient was 0.63 and 0.71 in IQ210-60 and IQ210-180 specimens, respectively. The rate of increase in the coefficient of friction in these specimens slowed down with increasing isothermal holding time. This may be due to the fact that the soft ferrite phase is more dominant in the microstructure with the growth of the precipitated carbides after the bainite transformation is completed. Since the ferrite phase in the microstructure has an adhesive effect on the sliding counter material, it has led to an increase in the friction coefficient.

The wear rate graph of the specimens is given in Fig. 10. The wear rate increased with the isothermal holding time and temperature. It can be noted that the wear rate variations are not related to the hardness values of all specimens. The wear rate increased with increasing isothermal temperature and holding time.

The least wear rate was obtained in the IQ210-90 specimen by applying mar-quenching process. With the initiation of the lower bainitic transformation at 210°C, the wear rate increased relatively. With the processes performed at 350 and 400°C, where the upper bainitic transformation took place, the hardness value of the specimens decreased significantly, resulting in an increase in the wear rate. As expected, the wear rate increased higher in the specimens with the lowest hardness IQ400-90 and IQ400-180. Frequently, while the friction coefficient decreases, the wear rate decreases, although the friction coefficient is low in the specimens annealed at 400°C, the wear rate increases. As a possible reason for this, while the coarser precipitated Fe_3C particles decreased the friction coefficient, they could be broken during friction with the encounter material, increasing the wear rate.

In Fig. 12, worn SEM surface images of the specimens are given. As seen in Fig. 12a, the wear tracks on the worn surface of the IQ210-90 specimen annealed at low isothermal temperature appear very thin, shallow and smoother.

By the martempering process, it is understood that in this specimen, which has the highest hardness value and the lowest wear rate, less wear debris is removed from the worn surface. When the holding time is increased at this temperature, partial adhesive wear tracks indicated by orange arrow on SEM image are observed on wear surfaces due to the relative decrease in hardness as a result of bainitic transformation, as in
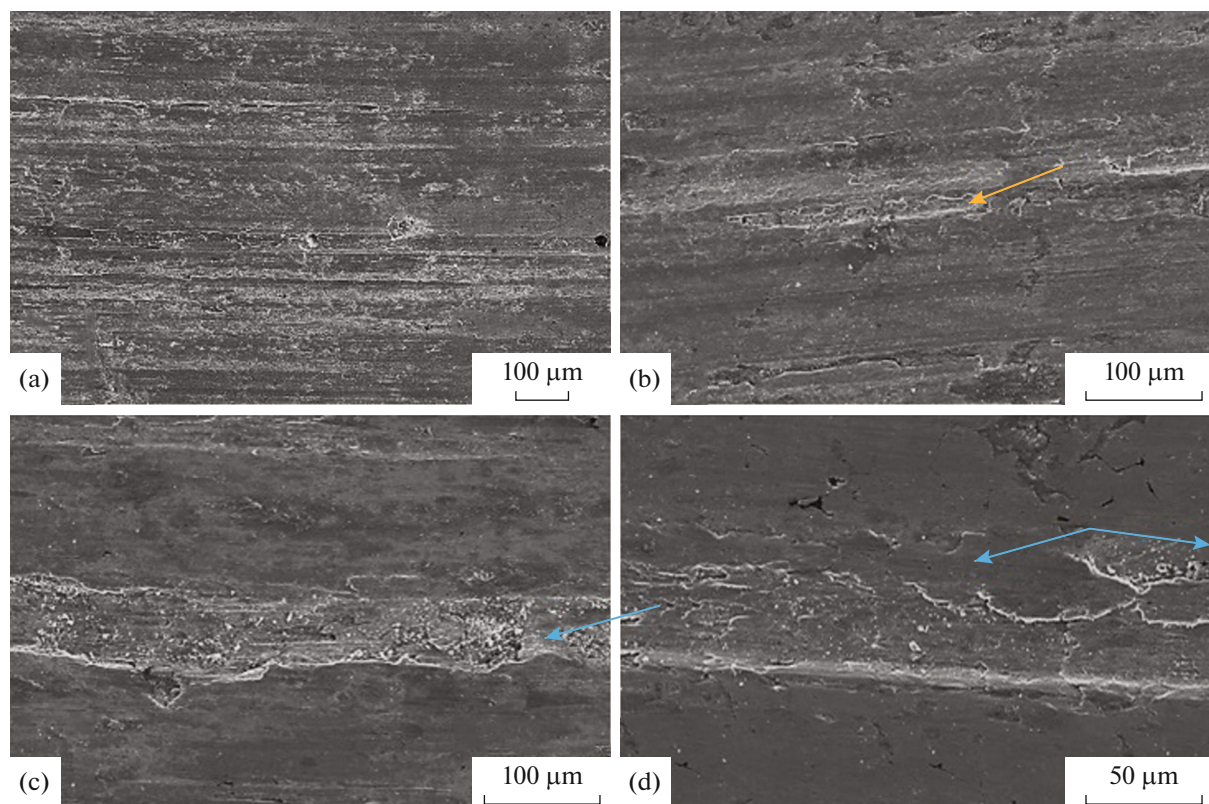
Fig. 12. Worn surface SEM images of (a) IQ210-90, (b) IQ210-360, (c) IQ350-60 and (d) IQ400-60 specimens.

the IQ210-360 specimen (Fig. 12b). As seen in Figs. 12c and 12d, respectively, in the IQ350-60 and IQ400-60 specimens, adhesive wear tracks are much more evident on the wear surfaces due to the much lower hardness value. When upper bainite is produced in the microstructure, traces of delamination resulted in a higher wear rate which can be seen on wear surfaces as a result of the adhesive effect indicate by blue arrows.

CONCLUSIONS

(1) As quenched P/M sample, while the typical plate martensitic microstructure was produced. Internal cracks were formed in the martensite plates due to the high carbon content. In addition, according to XRD analysis, the presence of retained austenite was observed in the directly quenched samples. With the increase of isothermal annealing time and temperature, retained austenite peaks disappeared.

(2) The hardness values of the samples decreased with the increase of isothermal annealing temperature and holding time. While the highest hardness value was 370 HV1 in the specimen, which was annealed 90 s at 210°C, the hardness decreased to 340 HV1 by isothermal holding time for 360 s. When the isother-

mal annealing temperatures were increased for the austempering process, the hardness values decreased and the lowest hardness was achieved at the end of the 60 s isothermal holding time at 400°C with 315 HV1 value. The possible reason is the increase in the bainitic transformation with the decrease of the martensite volume ratio with the increase of both the annealing temperature and the holding time.

(3) The increase in the isothermal holding time of the samples increased both the friction coefficient and the wear rate. However, it was seen that the friction coefficient of the specimens was not directly related to the hardness. The friction coefficient of the specimen with the lowest hardness, which was treated isothermal at 400°C, is lower than the specimens with higher hardness. The reason for this is thought to decrease the wear disc contact area of hard Fe_3C particles precipitated due to the formation of upper bainite at 400°C.

CONFLICT OF INTEREST

The authors of this work declare that they have no conflicts of interest.

REFERENCES

1. M. Carsí, A. F. Fernández-Vicente, O. A. Ruano, and O. D. Sherby, "Processing, microstructure, strength, and ductility relationships in ultrahigh carbon steel assessed by high strain rate torsion testing," Mater. Sci. Technol. **15**, 1087−1095 (1999).
https://doi.org/10.1179/026708399101506814

2. M. D. Hecht, Yo. N. Picard, and B. A. Webler, "Effects of Cr concentration on cementite coarsening in ultra-high carbon steel," Metall. Mater. Trans. A **50**, 4779−4790 (2019).
https://doi.org/10.1007/s11661-019-05403-w

3. M. D. Hecht, Yo. N. Picard, and B. A. Webler, "Coarsening of inter- and intra-granular proeutectoid cementite in an initially pearlitic 2C−4Cr ultrahigh carbon steel," Metall. Mater. Trans. A **48**, 2320−2335 (2017).
https://doi.org/10.1007/s11661-017-4012-2

4. W. Liu, Ya. Cao, Yi. Guo, B. Xu, M. Sun, and D. Li, "Characteristics and transformation of primary carbides during austenitization in Cr_4Mo_4V bearing steel," Mater. Charact. **169**, 110636 (2020).
https://doi.org/10.1016/j.matchar.2020.110636

5. W. M. Melfo, R. J. Dippenaar, and B. J. Monaghan, "Effect of particle composition on consolidation of hot briquetted iron," Ironmaking Steelmaking **33**, 93−100 (2006).
https://doi.org/10.1179/174328106x80118

6. T. V. S. Rajan, C. P. Sharma, A. K. Sharma, et al., *Heat Treatment: Principles and Techniques* (PHI Learning, New Delhi, 2011).

7. V. M. Schastlivtsev, Yu. V. Kaletina, E. A. Fokina, and A. Yu. Kaletin, "Effect of cooling rate on the amount of retained austenite upon bainitic transformations," Phys. Met. Metallogr. **115**, 990−1000 (2014).
https://doi.org/10.1134/s0031918x14100147

8. P. V. Krishna, R. R. Srikant, M. Iqbal, and N. Sriram, "Effect of austempering and martempering on the properties of AISI 52100 steel," ISRN Tribol. **2013**, 515484 (2013).
https://doi.org/10.5402/2013/515484

9. M. H. Shaeri, H. Saghafian, and S. G. Shabestari, "Effect of heat treatment on microstructure and mechanical properties of Cr−Mo steels (FMU-226) used in mills liner," Mater. Des. **34**, 192−200 (2012).
https://doi.org/10.1016/j.matdes.2011.07.042

10. Yu. Lin, Ya. Zheng, Z. Wu, and W. Garrison, "A discussion of the effects of composition and heat treatment on the toughness of a medium carbon secondary hardening steel," Mater. Sci. Eng., A **748**, 213−227 (2019).
https://doi.org/10.1016/j.msea.2019.01.079

11. Y. Shigeta, M. Aramaki, K. Ashizuka, Y. Ikoma, and Y. Ozaki, "Effect of networked Cu-rich ferrite phase on proof stress and ultimate tensile strength of sintered bodies of Fe−Cu hybrid-alloyed steel powder with graphite," Powder Metall. **64**, 134−141 (2021).
https://doi.org/10.1080/00325899.2021.1871805

12. R. M. German, *Powder Metallurgy Science* (Metal Powder Industries Federation, United States, 1984).

13. O. Altuntaş and A. Güral, "Designing spherical cementite in bainitic matrix (SCBM) microstructures in high carbon powder metal steels to improve dry sliding wear resistance," Mater. Lett. **249**, 185−188 (2019).
https://doi.org/10.1016/j.matlet.2019.04.095

14. P. C. Angelo and R. Subramanian, *Powder Metallurgy: Science, Technology and Applications* (PHI Learning, New Delhi, 2008).

15. *Advances in Powder Metallurgy: Properties, Processing and Applications*, Ed. by I. Chang and Y. Zhao, Woodhead Publishing Series in Metals and Surface Engineering (Woodhead Publishing, 2013).
https://doi.org/10.1533/9780857098900

16. M. H. Elahinia, M. Hashemi, M. Tabesh, and S. Bhaduri, "Manufacturing and processing of NiTi implants: A review," Prog. Mater. Sci. **57**, 911−946 (2012).
https://doi.org/10.1016/j.pmatsci.2011.11.001

17. M. Steeper, M. Jackson, P. Madin, and K. Ridal, "Advances in metal manufacturing technologies," Ironmaking Steelmaking **38**, 241−249 (2011).
https://doi.org/10.1179/030192311x13001032135164

18. P. Burke, C. Petit, V. Vuaroqueaux, A. Doyle, and G. Kipouros, "Processing parameters and post-sintering operations effects in magnesium powder metallurgy," Can. Metall. Q. **50**, 240−245 (2011).
https://doi.org/10.1179/1879139511y.0000000013

19. S. Tekeli and A. Güral, "Microstructural characterisation of intercritically annealed 0.5 wt−%Ni and Mn added steels prepared by powder metallurgy method," Mater. Sci. Technol. **23**, 72−78 (2007).
https://doi.org/10.1179/174328407x158442

20. M. Khaleghi and R. Haynes, "Sintering and heat treatment of steels made from a partially prealloyed iron powder," Powder Metall. **28**, 217−223 (1985).
https://doi.org/10.1179/pom.1985.28.4.217

21. K. S. Narasimhan, "Sintering of powder mixtures and the growth of ferrous powder metallurgy," Mater. Chem. Phys. **67**, 56−65 (2001).
https://doi.org/10.1016/s0254-0584(00)00420-x

22. L. A. Dobrzański, G. Matula, A. Várez, B. Levenfeld, and J. M. Torralba, "Fabrication methods and heat treatment conditions effect on tribological properties of high speed steels," J. Mater. Process. Technol. **157-158**, 324−330 (2004).
https://doi.org/10.1016/j.jmatprotec.2004.09.051

23. S. Geroldinger, R. de Oro Calderon, C. Gierl-Mayer, and H. Danninger, "Sinter hardening PM steels prepared through hybrid alloying," HTM J. Heat Treat. Mater. **76**, 105−119 (2021).
https://doi.org/10.1515/htm-2020-0007

24. S. S. Rathore and V. V. Dabhade, "Hardenability of sinter-forged Fe−2Cu−0.7C−xMo alloys," J. Alloys Compd. **664**, 133−140 (2016).
https://doi.org/10.1016/j.jallcom.2015.12.240

25. S. Chatterjee and H. K. D. H. Bhadeshia, "TRIP-assisted steels: Cracking of high-carbon martensite," Mater. Sci. Technol. **22**, 645–649 (2006). https://doi.org/10.1179/174328406x86182

26. M. K. Bai, J. C. Pang, G. D. Wang, and H. L. Yi, "Martensitic transformation cracking in high carbon steels for bearings," Mater. Sci. Technol. **32**, 1179–1183 (2016). https://doi.org/10.1080/02670836.2016.1148108

27. S. Pashangeh, M. C. Somani, S. S. Ghasemi Banadkouki, H. R. Karimi Zarchi, P. Kaikkonen, and D. A. Porter, "On the decomposition of austenite in a high-silicon medium-carbon steel during quenching and isothermal holding above and below the Ms temperature," Mater. Charact. **162**, 110224 (2020). https://doi.org/10.1016/j.matchar.2020.110224

28. D. R. H. Jones and M. F. Ashby, *Engineering Materials 2: Forming of The Structure and Properties, Materials Selection*, 2nd ed. (WNT, 1998).

29. W. L. Costin, O. Lavigne, and A. A. Kotousov, "A study on the relationship between microstructure and mechanical properties of acicular ferrite and upper bainite," Mater. Sci. Eng., A **663**, 193–203 (2016). https://doi.org/10.1016/j.msea.2016.03.103

30. R. Hossain, F. Pahlevani, and V. Sahajwalla, "Stability of retained austenite in high carbon steel—Effect of post-tempering heat treatment," Mater. Charact. **149**, 239–247 (2019). https://doi.org/10.1016/j.matchar.2019.01.034

Publisher's Note. Pleiades Publishing remains neutral with regard to jurisdictional claims in published maps and institutional affiliations.